Feasibility Study of Using Active Microwave Data for Examination of Thaw Lake Drainage Patterns over the Yamal Peninsula

Anna Maria Trofaier, William Gareth Rees
Scott Polar Research Institute, University of Cambridge, Cambridge, UK

Annett Bartsch, Daniel Sabel, Stefan Schlaffer
Vienna University of Technology, Institute of Remote Sensing and Photogrammetry, Vienna, Austria

Abstract

The applicability of radar data for monitoring the seasonal changes in permafrost thaw lake surface extent on the Yamal Peninsula is investigated. Data from the European Space Agency's ENVISAT Advanced Synthetic Aperture Radar (ASAR) operating in wide swath mode are used to map water bodies by applying simple threshold classification algorithms. A change detection analysis of lake surface extent shows that there are inundation variations between seasons. These preliminary results allow for the identification of summer drainage of certain lakes. However, due to the sensor-related limitations, the reason for this seasonal lake drainage pattern cannot be established. We assume that the interplay between the lakes and rivers should be taken into account for a complete understanding of lake dynamics. This paper hopes to communicate that ENVISAT ASAR WS data can be successfully used in the first instance to identify hotspots of lake change.

Keywords: active microwave; remote sensing; Russia; thermokarst lakes; Yamal Peninsula.

Introduction

Landscape evolution is a natural process. Periglacial environments have undergone modifications throughout the Quaternary. Nonetheless, the current trend of increasing air temperatures is raising concerns about the implications these temperatures may have on permafrost landscapes in arctic and subarctic regions.

Thermokarst is a process related to the thawing of frozen ground in ground-ice-rich regions. Ground ice ablation results in topographic slumping, known as thermokarst subsidence. Thaw waters accumulate in the resulting depressions. These thaw waters are known as thermokarst lakes or ponds, depending on their respective sizes. Tundra thaw ponds are of limited size; their diameter often being below 2 km (French 2007).

Thermokarst lakes and ponds are abundant in arctic and subarctic regions; in particular they cover the vast tundra lowlands. They are subject to seasonal variations due to snowmelt and fluctuations in precipitation, both of which can lead to changes in lake extent. The interaction of water bodies with permafrost is crucial to permafrost hydrology. Water has a high heat capacity, which results in further ground thawing. Hence surface water itself and changes in its extent affect permafrost processes.

During recent decades, a warming trend in the upper permafrost layers has been observed in high-latitude regions (Romanovsky et al. 2010). This warming affects permafrost processes. We hypothesize that changes in permafrost terrain are not necessarily attributed to climate-induced landscape evolution. Seasonal effects, associated with distinct change patterns, also need to be considered. This study provides preliminary data of an ongoing investigation on changes in thermokarst lakes. The paper focuses on the technical aspect of using ENVISAT ASAR WS as a means of identifying lake change. The assumption is that frequent monitoring over consecutive years provides insight into any interannual variations in changes in lake extent.

Satellite data have been used in many studies to monitor lakes over the vast tundra regions. However, due to their limited size, tundra ponds are not captured in satellite-based global land cover datasets (Frey & Smith 2007, Bartsch et al. 2008). High spatial resolution data are required. Such data are available from optical sensors. The availability of acquisitions depends on daylight and cloud conditions. Aerial photographs are most suitable, but their availability is constrained due to acquisition difficulties. Satellite data provide an alternative means for more extensive archived material. Landsat data have been available since the 1970s, and multispectral instruments—the Thematic Mapper (TM) and, in later missions, the Enhanced Thematic Mapper (ETM)—have frequently been used to capture land cover changes in thermokarst regions (e.g., Frohn et al. 2005, Grosse et al. 2006, Ulrich et al. 2009, Arp et al. 2011). Other optical data are available for even longer periods back in time. Corona data, which date back to the 1960s, and the more recent Ikonos data have been of interest for permafrost studies (Yoshikawa & Hinzman 2003, Grosse et al. 2005). Less extensive archives for active microwave data are available. However, these sensors, such as synthetic aperture radar (SAR), are independent of cloud cover and illumination and have proved to be a useful method for providing observations and monitoring features of the hydrosphere (Bartsch et al. 2009). The feasibility of using radar for monitoring thermokarst lakes is explored in this study. In particular, our interest lies in exploiting active microwave data for the analysis of lake drainage patterns.

Representative data for the phenomenon of lake change are restricted to late summer acquisitions, since most lakes are often still frozen at the beginning of summer. Lake drainage and shrinkage have been reported based on optical satellite data from Alaska (Yoshikawa & Hinzman 2003), Siberia (Smith et

al. 2005), and Canada (Plug et al. 2008, Labreque et al. 2009). However, both decreasing and increasing lake surface extent are reported, depending on geographical location (Grosse et al. 2011).

The aim of this study is to analyze ENVISAT ASAR WS data of the Yamal Peninsula for the years 2007 to 2009, and to quantify the magnitude of changes in lake surface extent that are identified by the sensor. This paper evaluates the use of ENVISAT ASAR WS and discusses the implications of strategies of thermokarst monitoring with satellite data.

Study Area

The topography of the Yamal Peninsula is a ground-ice-rich lowland with gently rolling hummocky terrain; it is a typical thermokarst landscape. The greatest elevation on the Yamal Peninsula is about 40 m a.s.l. (Mahaney et al. 1995). Numerous streams meander through this landscape, many of which lie below the spatial resolution of ENVISAT ASAR operating in wide swath mode. These streams are to be kept in mind because the interactions between lakes and the river systems may play a key role in lake dynamics.

The focus has been on two study areas where changes in lake extent are identified by the sensor. One is located near the Bovanenkovo gas field in the west of the Yamal Peninsula (ROI 1). The other area lies south of this (ROI 2). Both regions are indicated in Figure 1. Stratified silts and organic materials containing fibrous peat are found in these areas (Mahaney et al. 1995).

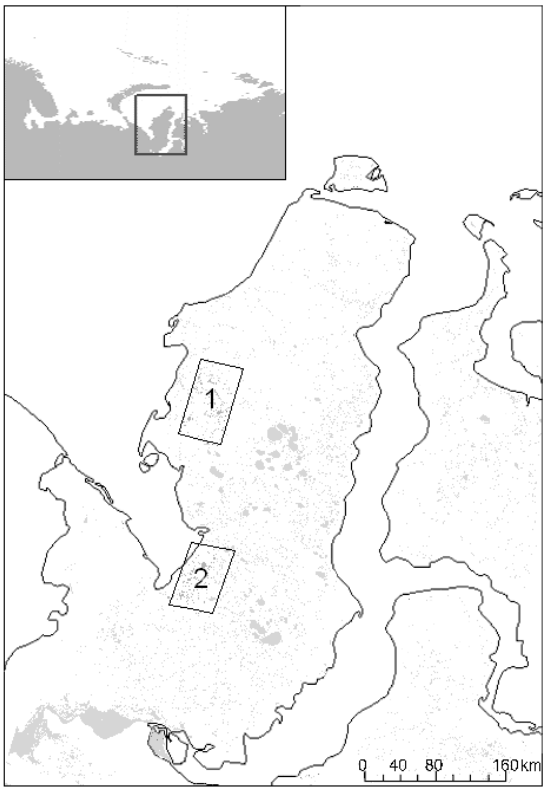

Figure 1. Map of the Yamal Peninsula. Grey areas represent ASAR WS classified water bodies, many of which fall below the map resolution.

Materials and Methods

Satellite data

This study uses data from the European Space Agency's ENVISAT Advanced Synthetic Aperture Radar (ASAR) instrument operating in wide swath (WS) mode. ASAR data have been collected since 2003 at several modes. In wide swath, which is a ScanSAR mode, a high number of images are available for certain areas in the Arctic, although not at regular intervals, and the data are acquired only on request. ASAR is a C-band sensor which has a center frequency of 5.331 GHz. The spatial resolution for ASAR WS is 150 m. This is rather coarse, but it allows improved mapping over larger regions and the majority of tundra ponds are captured (Bartsch et al. 2008). The data for this study were taken in HH polarization.

The first few stages in the processing chain are usually referred to as pre-processing steps. These can be divided into calibration and georeferencing, where the former encompasses the conversion of the raw digital numbers, which are measured by the sensors, into their representative physical quantities (Rees 2006). The pre-processing steps are as follows:

1. Radiometric calibration
2. Geometric correction
3. Normalization - Local incidence angle correction

Advanced data handling is required for change detection applications, which rely on a high number of samples. The datasets are resampled to pre-defined tiles (Pathe et al. 2009, Sabel et al. in press), and single acquisitions are stored as layer stacks. Only datasets from the snow- and freeze-free period have been selected. Snowmelt is usually complete by mid-June over the Yamal Peninsula (Bartsch 2010).

Inundation mapping

The method of thresholding is applied to the ASAR WS data for classification purposes. Specular reflection of the radar beam at the air-water interface of lakes on wind-free days allows for a clear distinction of water from the surrounding neighborhood. The backscatter value of a lake with low surface roughness (i.e., for low wind conditions) in an ASAR normalized image is about -14 dB, when normalized to an incidence angle of 30° (Bartsch et al. 2011). This backscatter value is set to be the threshold.

An automated classification of the summer months July and August in each year is done on a fortnightly basis. The classification routine is set to identify any pixels that lie below the aforementioned threshold, which are then classified as water pixels. In a post-processing step, a further condition is introduced: at least two ASAR measurements within the given time period for each pixel. Hence four classifications for each year, two in each month, are established. The classification details are given in Table 1. This classification method provides a means for identifying lake surfaces at their greatest extent within a two-week period.

Table 1. Classifications.

Classification	Time period for each year	
	Start date	End date
A	01 July	14 July
B	15 July	31 July
C	01 August	14 August
D	15 August	31 August

Table 2. Number of ENVISAT measurements for each classification.

Classification	Maximum number of images used for ROI 1			Maximum number of images used for ROI 2		
	2007	2008	2009	2007	2008	2009
A	12	14	4	8	13	3
B	15	14	9	13	12	7
C	12	9	8	11	7	8
D	13	11	7	10	8	4

Change detection

The classification procedure is then followed by a Geographic Information System (GIS) lake surface analysis as a means of change detection. This is done by subtracting each classification from its temporally preceding classification, thereby arriving at three classifications for changes that have occurred over July and August (classification A-B, B-C, and C-D).

Optimum threshold sensitivity analysis

The classification procedure is dependent on the chosen threshold of -14 dB. This threshold is selected in accordance with previous studies that have explored the threshold approach and found it to produce satisfactory results (Bartsch et al. 2007, Bartsch et al. 2008). Nonetheless, an optimum threshold evaluation for a set of randomly chosen lakes is performed for further sensitivity analysis of the water pixel classification to the chosen threshold.

This procedure was done in the ImageJ software environment (Abramoff et al. 2004). The optimum threshold for a set of 12 randomly selected lakes for five ASAR WS images was determined manually. The software was then used to calculate the area and perimeter of each lake. The error in the threshold value was investigated by analyzing the change in mean lake diameter and area as a function of threshold value.

Results

There are two regions on the Yamal Peninsula where larger variations are identified by the sensor. The first region of interest (ROI 1) is situated in the northwest of the Yamal Peninsula. The Bovanenkovo gas field lies in the north within ROI 1. The second region of interest (ROI 2) is located south of ROI 1. Both regions are shown in Figure 1, and their geographical coordinates are given in Tables 3 and 4.

Table 3. Geographic coordinates for ROI 1.

Corner points	Latitude (N)	Longitude (E)
Upper left	70°30′ 1.744″	67°53′ 59.15″
Lower right	69°48′ 5.265″	68°59′ 57.25″

Table 4. Geographic coordinates for ROI 2.

Corner points	Latitude (N)	Longitude (E)
Upper left	68°35′ 60.00″	68°44′ 52.82″
Lower right	67°56′ 11.99″	69°32′ 43.23″

The manually determined optimum threshold for each lake in each image showed that this optimum threshold varied significantly from lake to lake and was also image dependent. The values range from -15 to -9.8 dB. The standard deviation of the entire set of optimum threshold values was found to be 1.22 dB. It was therefore decided to proceed with a threshold sensitivity analysis in steps of 1 dB.

The sensitivity analysis of the threshold conditions showed that an increase in threshold by 1 dB results in an average change in mean lake diameter of ~21.84 m. The choice of using a threshold value that is at the lower end of the optimum threshold range is related to the loss in separability of the lakes from the surrounding neighborhood. At a threshold of -10 dB, most of the selected lakes merge with neighboring lakes. In addition, the increase in noise from pixels that are classified as water but cannot be identified as lakes, due to spatial resolution constraints, provides the reasoning for setting the threshold value at -14 dB.

The total pixel count change for each classification is shown in Figure 4. The total change can be divided into changes due to pixel loss versus pixel gain. A map of lake change due to loss in pixel count is given in Figure 2.

Pixel count of lake area is highly dependent on the number of measurements available from ENVISAT ASAR for each classification. Figure 3 shows the pixel count for each classification of ROI 1 in 2007 as a function of ASAR measurements.

The cumulative changes in water pixel count for ROI 1, for both loss and gain, are given in Figure 5, where loss and gain in pixel count are represented by negative and positive values, respectively. The greatest change in loss in both regions occurs between the first two classifications. In each case, loss in water pixel count decreases steadily thereafter. This holds for ROI 1. Similarly, this behavior is also found for ROI 2 in 2007. Unfortunately, the number of measurements available that meet the threshold conditions was greatly limited in 2008 and 2009 for ROI 2.

The bottom right panel of Figure 2 shows the water pixel counts for each classification in 2008 for ROI 2 as a function of ASAR measurements.

In addition to loss, the gain in water pixel count was also identified. This gain is primarily around the margins of the water bodies and could be attributed to mixed pixels.

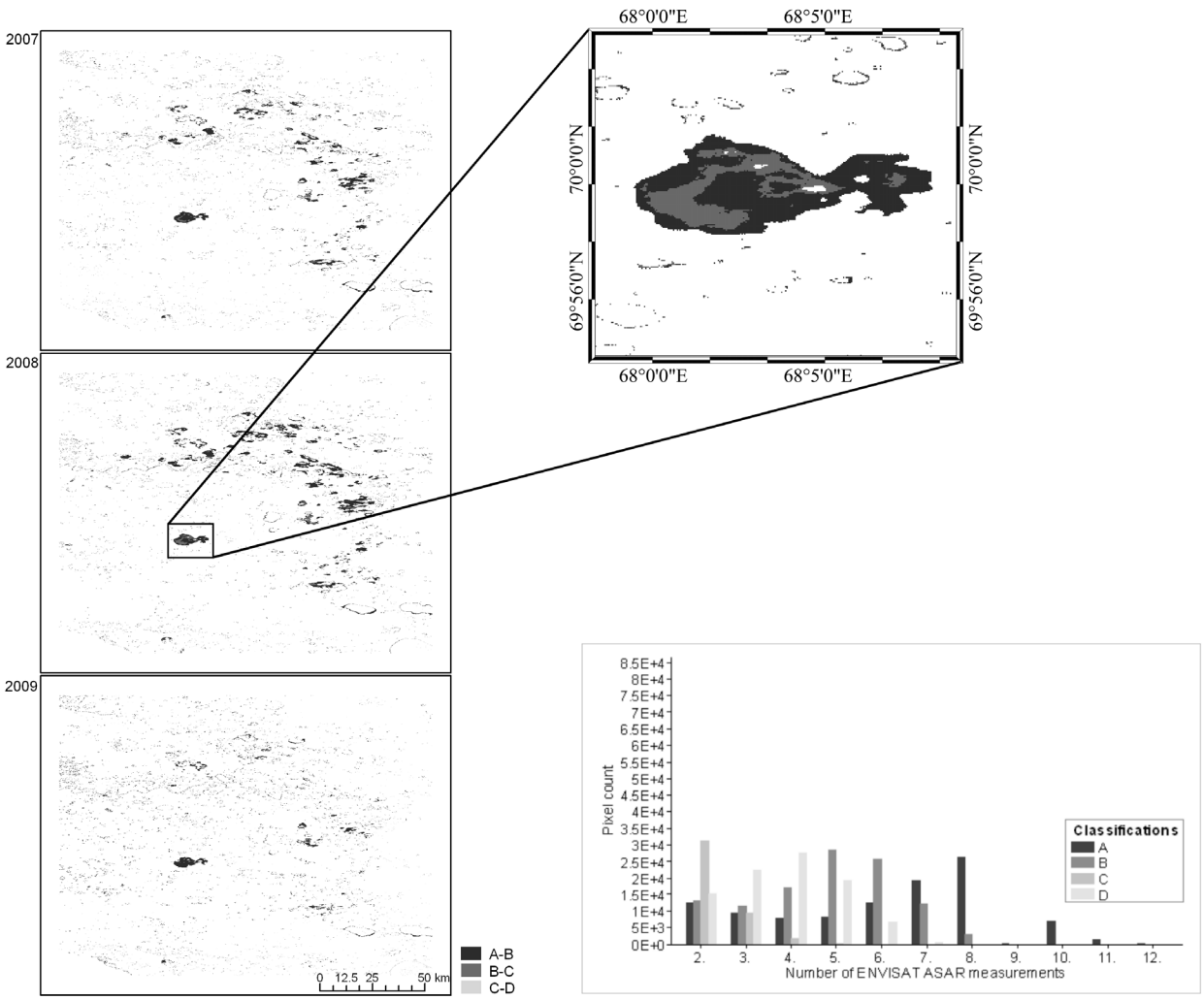

Figure 2. Map of water pixel loss for ROI 1 (left). Number of measurements and associated pixel count for each classification for ROI 2 in 2008 (bottom right).

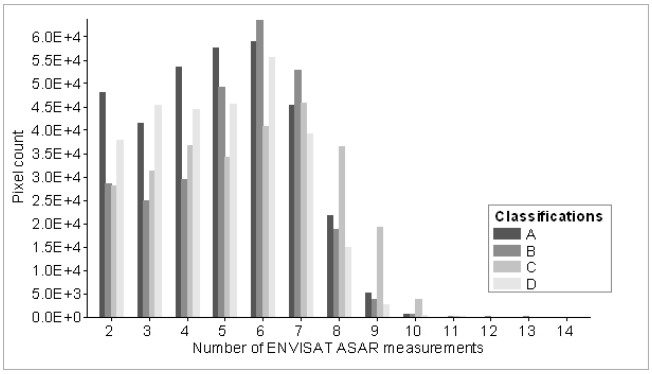

Figure 3. Number of measurements and associated pixel count for each classification for ROI 1 in 2007.

Furthermore, wind conditions seem to play a crucial role, in particular concerning large lakes. At high wind speed, an increase in the surface roughness of these lakes will result in loss of separability from their surroundings, and these data will not be classified as water bodies. The classifications, and hence the results for the change analysis, will be affected by this problem. Therefore, gain in lake extent is also associated with an increase in data (i.e., better wind conditions). This issue is particularly prominent in ROI 2 in both 2008 and 2009, as can be seen from the pixel counts for each classification depicted in the bottom panel of Figure 4.

Discussion

The ASAR WS analysis of lake surface extent on the Yamal Peninsula shows that there are two regions in which a sudden decrease in the number of water pixels in the first few weeks of July is visible. It is hypothesized that this is related to a distinct seasonal pattern in lake drainage, which may in turn result from river-lake interactions. However, due to spatial resolution constraints of the sensor, these interactions cannot be investigated by the current method. Further research into this phenomenon is necessary.

The automated thresholding approach is used as a time efficient means to produce a fairly accurate classification. The choice of threshold is at the lower end of the optimum threshold range of the random lake sample. However, our error investigation showed that given the great range of

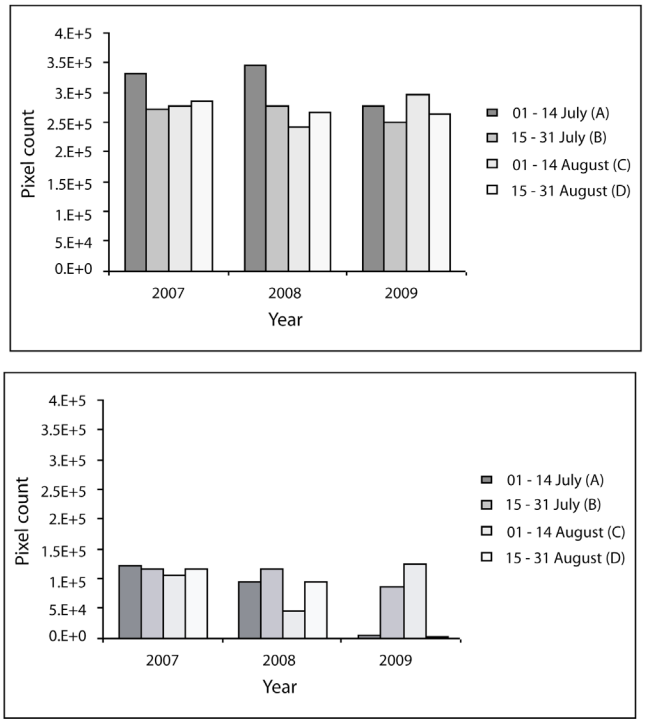

Figure 4. Pixel count of each classification for ROI 1 (top) and ROI 2 (bottom).

optimum thresholds and the lower signal to noise ratios at higher thresholds, the average change in mean lake diameter was sufficiently low to use a threshold value of -14 dB. Indeed, given the sensor's spatial resolution of 150 m and an average change in mean lake diameter of less than 22 m, the applicability of the thresholding approach is clearly justifiable.

The results show that the regular monitoring of these water bodies with the aid of ASAR WS is restricted by the impact of local wind conditions. The high variability of wind speed produces skewed classification results, which hinder a comprehensive analysis based solely on SAR data. Bartsch et al. (2011) have discussed the effects of wind on this classification technique. The classification problem is distinctly noticeable for ROI 2 in both 2008 and 2009, when the number of ASAR WS measurements is greatly limited.

These restrictions have implications for continuous monitoring of lake dynamics. Advanced knowledge of weather conditions from meteorological records provides complementary information and allows a pre-selection of wind-free datasets. However, such records are not always available. Further, this knowledge will have no impact on the number of ASAR WS measurements. The ASAR WS sensor is a highly capable device for frequent monitoring, but severe wind conditions common to high-latitude regions impinge on its temporal resolution.

Conclusions

This study addresses the use of active microwave data as a preliminary method for investigating seasonal patterns in inundation dynamics. Permafrost thaw lakes on the Yamal Peninsula are monitored with the aid of synthetic aperture radar. The information retrieved from such sensors can be translated into classifications of inundation extent. Changes in lake surface extent are examined; both loss and gain in water pixel counts are established. As with many remotely sensed studies, data availability (both sensor and weather-related) poses a more complex issue that needs to be tackled for effective monitoring.

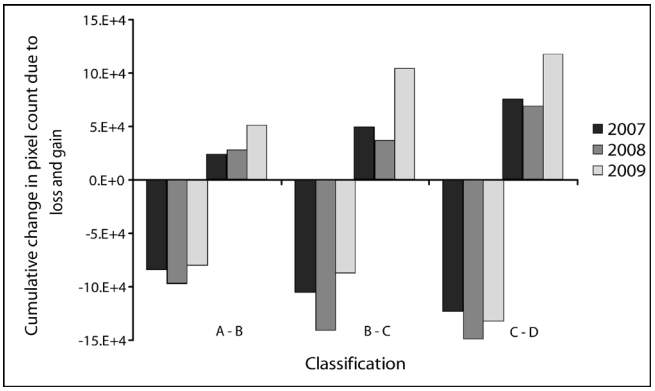

Figure 5. Cumulative change in pixel count due to water pixel loss and gain for ROI 1.

Acknowledgments

Satellite data processing has been supported by ESA initiatives DUE Permafrost (ESRIN Contr. No. 22185/09/I-OL) and STSE ALANIS-Methane (ESRIN Contr. No. 4000100647/10/I-LG). A.M. Trofaier is a recipient of a DOC-fFORTE-fellowship of the Austrian Academy of Sciences at the Scott Polar Research Institute. A. Bartsch has been a recipient of a research fellowship by the Austrian Science fund (FWF Elise Richter Program, V150- N21) during the course of the study.

References

Abramoff, M.D., Magalhaes, P.J., & Ram, S.J. 2004. Image Processing with ImageJ. *Biophotonics International* 11(7): 36-42.

Arp, C.D., Jones, B.M., Urban, F.E., & Grosse, G. 2011. Hydrogeomorphic processes of thermokarst lakes with grounded-ice and floating-ice regimes on the Arctic coastal plain, Alaska. *Hydrological Processes.*

Bartsch, A. 2010. Ten Years of SeaWinds on QuikSCAT for Snow Applications. *Remote Sensing* 2: 1142-1156.

Bartsch A., Kidd, R., Pathe, C., Wagner, W., & Scipal, K. 2007. Satellite radar imagery for monitoring inland wetlands in boreal and sub-arctic environments. *Journal of Aquatic Conservation: Marine and Freshwater Ecosystems* 17: 305-317.

Bartsch, A., Pathe, C., Wagner, W., & Scipal, K. 2008. Detection of Permanent Open Water Surfaces in Central Siberia with ENVISAT ASAR Wide Swath Data with Special Emphasis on the Estimation of Methane Fluxes from Tundra Wetlands. *Hydrology Research* 39: 89-100.

Bartsch, A., Trofaier, A.M., Hayman, G., Sabel, D., Schlaffer, S., Clark, D., & Blythe, E. 2011. Detection of wetland dynamics with ENVISAT ASAR in support of methane modeling at high latitudes. *Biogeosciences Discuss* 8: 8241-8268.

Bartsch, A., Wagner, W., Scipal, K., Pathe, C., Sabel, D., & Wolski, P. 2009. Global monitoring of wetlands - the value of ENVISAT ASAR global mode. *Journal of Environmental Management* 90:2226-2233.

French, H.M. 2007. *The Periglacial Environment*, 3rd edition. Chichester, John Wiley & Sons, 191 pp.

Frey, K. & Smith, L.C. 2007. How Well Do We Know Northern Land Cover? Comparison of Four Global Vegetation and Wetland Products with a New Ground-Truth Database for West Siberia. *Global Biogeochemical Cycles* 21: GB1016.

Frohn, R.C., Hinkel, K.M., & Eisner, W.R. 2005. Satellite remote sensing classification of thaw lakes and drained thaw lake basins on the North Slope of Alaska. *Remote Sensing of Environment* 97:116-126.

Grosse, G., Jorgenson, T., Walter, K., Brown, J., & Overduin, P.P. 2011. Vulnerability and Feedbacks of Permafrost to Climate Change. *EOS Transactions, American Geophysical Union* 92: 73-80.

Grosse, G., Schirrmeister, L., Kunitsky, V.V., & Hubberten, H.-W. 2005. The use of CORONA images in remote sensing of periglacial geomorphology: An illustration from the NE Siberian coast. *Permafrost and Periglacial Processes* 16: 163-172.

Grosse, G., Schirrmeister, L., & Malthus, T. 2006. Application of Landsat-7 satellite data and a DEM for the quantification of thermokarst-affected terrain types in the periglacial Lena-Anabar coastal lowland. *Polar Research* 25(1): 51-67.

Labreque, S., Lacelle, D., Duguay, C.R., Lauriol, B., & Hawkings, J. 2009. Contemporary (1951–2001) Evolution of Lakes in the Old Crow Basin, Northern Yukon, Canada: Remote Sensing, Numerical Modeling, and Stable Isotope Analysis. *Arctic* 62(2): 225-238.

Mahaney, W.C., Michel, F.A., Solomatin, V.I., & Hütt, G. 1995. Late Quaternary stratigraphy and soils of Gydan, Yamal and Taz Peninsulas, northwestern Siberia. *Palaeogeography, Palaeoclimatology, Palaeoecology* 113: 249-266.

Pathe, C., Wagner, W., Sabel, D., Doubkova, M., & Basara, J. 2009. Using ENVISAT ASAR Global Mode Data for Surface Soil Moisture Retrieval Over Oklahoma, USA. *IEEE Transactions on Geoscience and Remote Sensing* 47(2): 468-480.

Plug, L.J., Walls, C., & Scott, B.M. 2008. Tundra lake changes from 1978 to 2001 on the Tuktoyaktuk Peninsula, western Canadian Arctic. *Geophysical Research Letters* 35: L03502.

Rees, W.G. 2006. *Remote Sensing of Snow and Ice.* Cambridge, Taylor and Francis, 76 pp.

Romanovsky, V.E., Smith, S.L., & Christiansen, H.H. 2010. Permafrost thermal state in the polar Northern Hemisphere during the International Polar Year 2007–2009: A synthesis. *Permafrost and Periglacial Processes* 21: 106-116.

Sabel, D., Bartalis, Z., Wagner, W., Doubkova, M., & Klein, J.-P. 2011. Development of a Global Backscatter Model in support to the Sentinel-1 mission design. *Remote Sensing of Environment*, in press.

Smith, L.C., Sheng, Y., MacDonald, G.M., & Hinzman, L.D. 2005. Disappearing Arctic Lakes. *Science* 308: 1429.

Ulrich, M., Grosse, G., Chabrillat, S., & Schirrmeister, L. 2009. Spectral characterization of periglacial surfaces and geomorphological units in the Arctic Lena Delta using field spectrometry and remote sensing. *Remote Sensing of Environment* 113:1220-1235.

Yoshikawa, K. & Hinzman, L.D. 2003. Shrinking thermokarst ponds and groundwater dynamics in discontinuous permafrost near Council, Alaska. *Permafrost and Periglacial Processes* 14: 151-160.